



MariaAngela Meireles is logged in
[Logout](#)

[Browse](#) [Search](#) [My Settings](#) [Alerts](#) [Help](#)

Quick Search Title, abstract, keywords Author e.g. j s smith **Go**

Chemistry Preprint Archive

Volume 2002, Issue 3, March 2002, Pages 138-145

[Result list](#) | [previous](#) < 1 of 1 > [next](#)

[SummaryPlus](#)

[Full Text + Links](#)

[PDF \(122 K\)](#)

[View thumbnail images](#) | [View full size images](#)



[E-mail Article](#)



[Export Citation](#)

PREDICTIONS OF BRANCHED AND CYCLIC CHAIN PROPERTIES FROM LINEAR CHAIN PROPERTIES: MOLECULAR SIMULATION AND THERMODYNAMIC POLYMERIZATION THEORY

Marcio Paredes^{a,✉} and MAA Meireles

LASEFI - DEA / FEA - UNICAMP

Available online 24 August 2004.

Predictive and reliable methods to obtain thermodynamic properties of natural products are very important for food engineering process design, including supercritical extraction. In this work we have studied the prediction of thermodynamic properties based on the molecular structure, calculating properties of branched and cyclic molecules from linear chains properties. The thermodynamic model used is based on the thermodynamic polymerization theory (TPT), where the chain segments interact via the Square-Well potential. In the TPT approach, the properties of linear, cyclic, and branched homo-segment chains can be calculated from the non-bonded macroscopic segment properties and from the segment-segment radial distribution function at the contact point (RDF). For this reason, Monte Carlo Canonical simulations were performed to evaluate the RDF between different segment types in linear chains, and to obtain the branched and cyclic chain properties. In order to analyze the results, cyclic and branched paraffin properties were calculated from the properties of a homologue series of normal alkanes. The predictions for branched chain properties agree very well with the experimental data. For cyclic chains, the predictions of saturation pressures are reasonable, while the predictions for saturated liquid densities are not good.

Author Keywords: Chemical Engineering > Chemical Engineering; chemeng/0203001

Chemistry Preprint Archive

Volume 2002, Issue 3, March 2002, Pages 138-145

[Result list](#) | [previous](#) < 1 of 1 > [next](#)

[Browse](#) [Search](#) [My Settings](#) [Alerts](#) [Help](#)



[About ScienceDirect](#) | [Contact Us](#) | [Terms & Conditions](#) | [Privacy Policy](#)

Copyright © 2007 Elsevier B.V. All rights reserved. ScienceDirect® is a registered trademark of Elsevier B.V.

PREDICTIONS OF BRANCHED AND CYCLIC CHAIN PROPERTIES FROM LINEAR CHAIN PROPERTIES: MOLECULAR SIMULATION AND THERMODYNAMIC POLYMERIZATION THEORY

Marcio L.L. Paredes and M. Angela A. Meireles

LASEFI, Depart. de Eng. de Alimentos, Fac. Eng. Alim., Unicamp, Cx.P. 6121, 13083-970 Campinas, SP, Brazil, phone: 19 37884033; fax: 19 37884027; meireles@fea.unicamp.br

Keywords: branched chains, molecular simulation

Predictive and reliable methods to obtain thermodynamic properties of natural products are very important for food engineering process design, including supercritical extraction. In this work we have studied the prediction of thermodynamic properties based on the molecular structure, calculating properties of branched and cyclic molecules from linear chains properties. The thermodynamic model used is based on the thermodynamic polymerization theory (TPT), where the chain segments interact via the Square-Well potential. In the TPT approach, the properties of linear, cyclic, and branched homo-segment chains can be calculated from the non-bonded macroscopic segment properties and from the segment-segment radial distribution function at the contact point (RDF). For this reason, Monte Carlo Canonical simulations were performed to evaluate the RDF between different segment types in linear chains, and to obtain the branched and cyclic chain properties. In order to analyze the results, cyclic and branched paraffin properties were calculated from the properties of a homologue series of normal alkanes. The predictions for branched chain properties agree very well with the experimental data. For cyclic chains, the predictions of saturation pressures are reasonable, while the predictions for saturated liquid densities are not good.

Introduction

In food engineering process design, the thermodynamic properties of natural products are often required but many times these properties are not available. For this reason, it is interesting to have a reliable method to obtain the desired physical-chemical information based on the molecular structure alone. Although this objective is not easy to accomplish, some promising tools have successfully been used to obtain chain properties from structure and segment properties, such as the molecular simulation and the molecular based models [1-5].

Equations of state derived from the SAFT [1,2] model are useful for this purpose. The SAFT equation is based on the Wertheim's [6] first-order Thermodynamic Perturbation Theory (TPT), in which chain properties are calculated from segment properties and where the bond effect on the thermodynamic properties is related to the radial distribution function at the contact point (RDF) between the disconnected segments and the chain segments [7]. Following this idea, cyclic and branched chain properties may be calculated from segment properties and the RDF between the segments involved in the bonds.

In order to obtain the RDF between different types of segments, Monte Carlo (MC) Canonical simulations were performed. Different types of segments and restrictions to contact are shown in Figure 1: (a) disconnected spheres (solid gray), with no restriction to contact with other spheres (hachured); (b) terminal segments, with restriction to contact from one side (chain side); (c) internal segments, with restriction to contact from two sides (neighborhood sides).

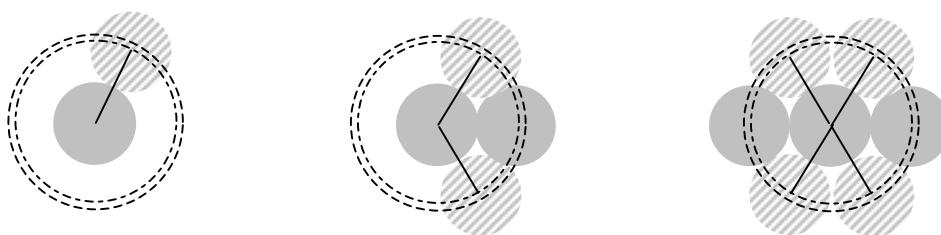


Figure 1. Two-dimension schematic representation of different segment types

The RDF of hard spheres and hard dumbbells can be calculated with the Carnahan-Starling [8] ($g_{1,1}$) and Chiew [9] ($g_{2,2}$) equations of state. From the TPT idea, it can be inferred that the RDF between disconnected spheres (1) and dumbbells segments (2), $g_{2,1}$, can be calculated as a geometric average of RDFs of same-type segments, as follows:

$$g_{2,1} = \sqrt{g_{1,1} \cdot g_{2,2}} = \sqrt{\frac{2-\eta}{2(1-\eta)^3} \cdot \frac{1+2\eta}{2(1-\eta)^2}} = \frac{1}{2(1-\eta)^2} \sqrt{\frac{(2-\eta)(1+2\eta)}{1-\eta}} \quad (1)$$

where η is the volume fraction occupied by the segments. In order to test this model, the predictions with the Carnahan-Starling (CS) and Chiew models and Eq. (1) were compared with the MC RDF simulations of Paredes *et al.* [5]. The results are in Figure 2 (a) and they show that the predictions with Eq. (1) are in excellent agreement with the simulation results. This idea is extended to square-well (SW) systems, with the well width (λ) equal to 1.5, as follows:

$$g_{2,1}^{\text{SW}} = \sqrt{g_{1,1}^{\text{SW}} \cdot g_{2,2}^{\text{SW}}} = \sqrt{g^{\text{SWS}} \cdot g^{\text{SWD}}} \quad (2)$$

where SWS denotes the square-well spheres and SWD denotes the square-well dumbbells.

The Tavares *et al.*'s models [3] have been used to calculate the RDF of the pure components in some reduced temperatures, $T^* = kT/\epsilon$, where k is the Boltzmann constant and ϵ is the interaction energy. The predictions with Tavares's models, Eq. (2) and MC simulations are plotted in Figures 2 (b) and 2 (c), and they show that the predictions with Eq. (2) are in excellent agreement with the simulation data, for both temperatures.

Although it is not so simple to infer from the TPT theory the relations between different types of segment, the geometric restrictions presented in Figure 1 together with equations (1) and (2) were used in this work to investigate models that predict the RDF between spheres, terminal and internal segments.

Materials and Methods

Radial Distribution Functions

In order to obtain the desired properties, some simplifications were made:

- The effect of the chain length on the RDF was neglected;
- The radial distribution functions that involve the same order of restrictions were considered as equal.

From these assumptions, the RDF between terminal segments was considered the same, not depending on the chain lengths. For this reason, the following equation may be written:

$$g_{t,t} = g_{t,2} = g_{2,2} \quad (3)$$

where t stands for terminal. In this case, there are two restrictions, one for each chain side of the terminal segment. In the RDF between disconnected segments and internal segments (i), there are also two restrictions, from the two chain sides of the internal segment. Following the simplifications,

$$g_{i,1} = g_{2,2} \quad (4)$$

In the calculation of the RDF between terminal and internal segments (3 restrictions), the arithmetic average between $g_{2,1}$ (1 restriction) and $g_{2,i}$ (3 restrictions) was used to give $g_{2,2}$ (2 restrictions).

$$g_{2,2} = \frac{g_{2,1} + g_{2,i}}{2} \therefore g_{2,i} = 2g_{2,2} - g_{2,1} \quad (5)$$

The same idea was used to calculate $g_{i,i}$ (4 restrictions).

$$g_{2,i} = \frac{g_{i,2} + g_{i,i}}{2} \therefore g_{i,i} = 2g_{i,2} - g_{2,2} = 3g_{2,2} - 2g_{2,1} \quad (6)$$

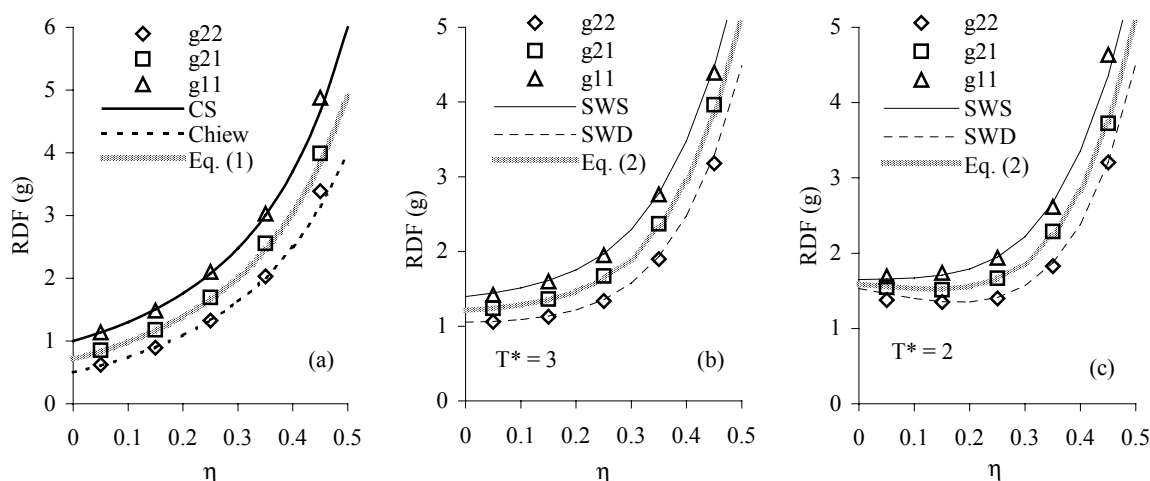


Figure 2. RDF from MC simulations [5] and models: (a) Hard spheres (g11) and hard dumbbells (g22), where CS and Chiew stand for Carnahan-Starling and Chiew models, (b) Square-well spheres (g11, SWS) and dumbbells (g22, SWD), where SWS and SWD stand for Tavares *et al.*'s models, with $T^* = 3$ and (c) The same as (b), with $T^* = 2$.

Thermodynamic Polymerization Theory

The idea presented here was used to calculate the linear chain properties with the TPT [6,7] model. In this theory, the chain properties are obtained from the properties of the dis-

connected spheres and from the effect of the connections on these properties. In the TPT theory, the connections are calculated as sphere-sphere connections, as follows:

$$Z^{\text{TPT1}} = 1 + m(Z_1 - 1) - (m - 1)\eta \frac{\partial}{\partial \eta} \ln g_{1,1} \quad (7)$$

where Z is the compressibility factor, Z_1 is the hard-sphere compressibility factor, and m is the number of segments in the chain. In the TPTD [7,10] model, dimers are formed and then connected to generate the same number of connections in the chain.

$$Z^{\text{TPTD}} = 1 + m(Z_1 - 1) - \frac{m}{2}\eta \frac{\partial}{\partial \eta} \ln g_{1,1} - \left(\frac{m}{2} - 1\right)\eta \frac{\partial}{\partial \eta} \ln g_{2,2} \quad (8)$$

Here it is proposed a new TPT model, in which two spheres are connected to form a dimer and then they are connected in the terminal segments of the chain:

$$Z^{\text{TPTN}} = 1 + m(Z_1 - 1) - \eta \frac{\partial}{\partial \eta} \ln g_{1,1} - \sum_{k=2}^{m-1} \eta \frac{\partial}{\partial \eta} \ln g_{k,1} \quad (9)$$

Using Eq. (3), Eq. (8) can be simplified, as follows:

$$Z^{\text{TPTN}} = 1 + m(Z_1 - 1) - \eta \frac{\partial}{\partial \eta} \ln g_{1,1} - (m - 2)\eta \frac{\partial}{\partial \eta} \ln g_{2,1} \quad (10)$$

Although Eqs. (8) and (10) are conceptually different, they become mathematically identical using Eq. (1). Applying the idea to attractive spheres, Eq. (2) also leads to the mathematical identity between the TPTN and the TPTD models.

Properties of Rings and Branched Chains

In spite of Eq. (10) being constructed for linear chains, the idea behind the model may be used to calculate ring properties by adding one connection between the terminal segments. Using the simplification presented in Eq. (3), the equation for rings becomes simply

$$Z^{\text{TPTN}} = 1 + m(Z_1 - 1) - \eta \frac{\partial}{\partial \eta} \ln g_{1,1} - (m - 2)\eta \frac{\partial}{\partial \eta} \ln g_{2,1} - \eta \frac{\partial}{\partial \eta} \ln g_{2,2} \quad (11)$$

For branched chains, the connections related to the branches have to be added, following the procedure used to add terminal-terminal connections in rings. For example, the equation for an m -segments linear chain with one branch is

$$Z^{\text{TPTN}} = 1 + (m + 1)(Z_1 - 1) - \eta \frac{\partial}{\partial \eta} \ln g_{1,1} - (m - 2)\eta \frac{\partial}{\partial \eta} \ln g_{2,1} - \eta \frac{\partial}{\partial \eta} \ln g_{2,2} \quad (12)$$

Monte Carlo Canonical Simulations

In order to evaluate the simplifications involved in Eqs. (3) to (6), MC simulations were performed and the desired properties were obtained from a mixture of tetramers (4 segments),

dimers (2 segments) and monomers (1 segment). The terminal tetramer segments are designated in the text by “4t” and the internal segments by “4i”. The simulations were carried out with 100 tetramer molecules, 100 dimer molecules and 200 monomer molecules. The initial configurations were generated with random segment positions (respecting the connections). The simulation consisted of equilibrium cycles (until the system reached equilibrium properties, from 10000 to 40000, depending on the volume fraction) and evaluation cycles (40000, in which the properties and deviations were calculated).

Model for Real Substances

In order to use this model to correlate real substance properties, the Barker-Henderson perturbation theory (BHPT) was used to calculate the properties of square-well chains with variable well widths. The models of Tavares *et al.*'s for the RDF of monomers and dimers were not used here to describe properties of real substances because these models are limited to $\lambda = 1.5$. The second-order BHPT was used to calculate Z_1 . For $g_{1,1}$, the first-order BHPT logarithmic expansion was used, as follows:

$$\ln(g_{1,1}^{sw}) = \ln(g_{1,1}) + \frac{1}{T^*} \frac{g_I}{g_{1,1}} \quad (13)$$

where g_I is a perturbation function. An empirical expression is proposed for $g_{2,2}$, based on Eq. (13) and on the simulation results of Paredes *et al.* [5]. The expression is

$$\ln(g_{2,2}^{sw}) = \ln(g_{2,2}) + \frac{1}{T^*} \frac{g_{II}}{g_{2,2}} = \ln(g_{2,2}) + \frac{1}{T^*} \frac{g_I + 0.3}{g_{2,2}} \quad (14)$$

where the value 0.3 arises from an average difference between g_{II} and g_I .

Results

Model x Simulation

Figure 3 (a) shows the MC simulation results for the RDF between different types of segments and the predictions with Eqs. (3) to (6). These results show that the predictions agree quite well with the simulation data, except for the predictions of $g_{4i,4i}$. In addition, for the small chains used here the simplifications do not lead to any serious limitation to the model.

The predictions with the TPTN equation for rings, Eq. (11), are compared to the simulation results of Lin *et al.* [11] for the compressibility factor of 16 and 32-segments rings. The results are plotted in Figure 3 (b) and they indicate that the model predictions agree very well with the simulation data.

Model x Real Substances Properties

In Table 1 the parameters obtained for some alkanes are presented. For the normal alkanes homologue series, the segment parameters ($\epsilon/k, \lambda, \sigma$) are almost equal for all substances, while the number of segments varies linearly with the number of carbons (n) in the chains, which is well represented by

$$m_{n\text{-alkane}} = 1.4 + 0.7 n \quad (15)$$

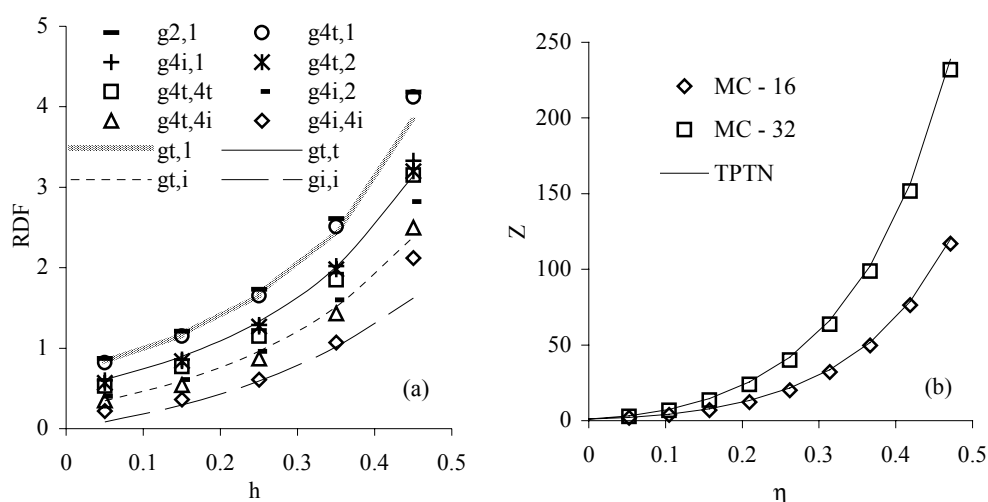


Figure 3. Comparison between the prediction with the proposed models and the MC simulation data: (a) Simulations obtained in this work and the prediction of the RDF between different types of segments and (b) Compressibility factor for 16 and 32-segment rings, with MC simulation [11] and TPTN prediction.

Branched Chains

In order to test the efficiency of Eq. (12), the isooctane saturation pressure and its liquid density were calculated and compared with experimental data [12] and with the correlation obtained from Eq. (10). Since isooctane is formed by a seven-carbon primary chain with one branch, the *n*-heptane parameters were used in this prediction. The properties are plotted in Figure 4. The prediction results are in very good agreement with the experimental data, with almost no difference from the correlation results. Similar results can be obtained in the prediction of isopentane properties.

Cyclic Chains

The saturation properties of cyclohexane were calculated with Eq. (11) and compared with the correlation with Eq. (10) and with experimental data [12]. The results are plotted in Figure 5. This substance is formed by six CH_2 groups, and so the properties of this group were used to calculate the cyclohexane properties. From Eq. (15) it can be inferred that each CH_2 group is related to 0.7 segments. The CH_2 group properties were assumed to be equal to the *n*-dodecane segments parameters, an alkane so lengthy that the influence of the terminal hydrogens could be neglected. Therefore, the cyclohexane parameters are the segment parameters of dodecane and $m = 6 * 0.7 = 4.2$. Figure 5 (a) shows that the predictions using Eq. (11) agree very well with the experimental data. However, this is not the case for the predictions of saturated liquid density, plotted in Figure 5 (b). Similar results can be obtained in the prediction of the cyclopropane properties, but with worse results for both properties.

Conclusions

In this work, the properties of branched and cyclic chains were studied. In order to calculate the desired properties, a new TPT-based model was proposed. Within the assumptions made, the model is mathematically equivalent to the TPTD model for linear chains. The simplifications in the evaluation of the radial distribution function at the contact point between different types of segments were tested against Monte Carlo Canonical simulations for hard chain mixtures. Although the proposed models are extremely simple, for the purpose of this

work the comparison with simulation data indicates no serious limitation. In order to use the model to describe the properties of real substances, the Square-Well potential was used and an empirical model for the square-well dimer radial distribution function was presented, based on molecular simulation results. The equation of state parameters were determined for an n-alkane homologue series, from ethane to dodecane, and almost constant segment parameters were obtained. The parameters for n-alkanes were used in the models to calculate the saturation pressure and the liquid density of isooctane and cyclohexane. The predictions agree quite well with the experimental data, except for the cyclohexane liquid density. The results indicate that the proposed approach is a good way to determine properties of complex substances, usually present in natural products.

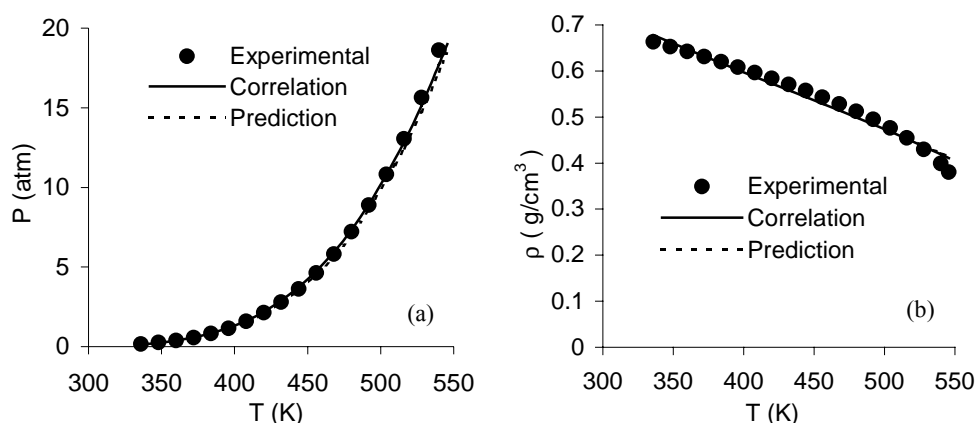


Figure 4. Isooctane saturation properties. Comparison between experimental [12] data, model correlation with Eq. (10) and prediction using Eq. (12) for: (a) Saturation Pressure and (b) Saturated Liquid Density.

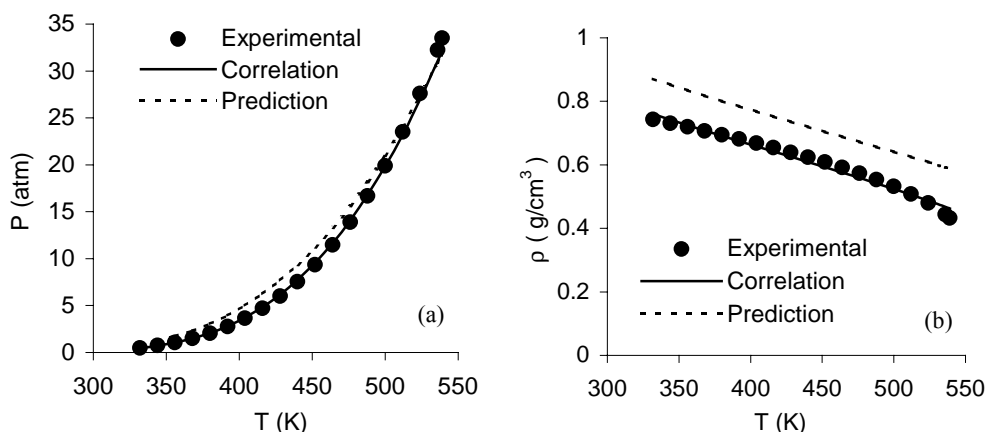


Figure 5 – Cyclohexane saturation properties. Comparison between experimental [12] data, model correlation with Eq. (10) and prediction using Eq. (11) for: (a) Saturation Pressure and (b) Saturated Liquid Density.

Table 1: Alkane parameters estimated using Eq. (10) with smoothed experimental data [12]. ϵ/k and λ are the square-well interaction energy and width, σ is the segment diameter and m is the number of chain segments. n, i, and c stand for normal, iso and cyclic. RMSD stands for root-mean-square, P for pressure and ρ for density.

Alkane	ϵ/k (K)	σ (Å)	λ	m	RMSDP ^{*1}	RMSD ρ ^{*2}
n - C ₂	80.0393	2.7669	1.8794	2.7354	1.53	2.32
n - C ₃	79.1223	2.7966	1.9294	3.4922	1.88	2.36
n - C ₄	80.8977	2.8309	1.9523	4.1503	2.28	2.52
n - C ₅	77.9796	2.8205	1.9855	4.9451	2.59	2.71
n - C ₆	79.3711	2.8449	1.9931	5.5783	2.62	2.66
n - C ₇	82.8972	2.8696	1.9848	6.1878	2.66	2.53
n - C ₈	79.8486	2.8427	2.0050	7.0416	3.02	2.70
n - C ₉	78.1651	2.8222	2.0175	7.8924	3.40	2.79
n - C ₁₀	79.5061	2.8385	2.0163	8.5007	3.27	2.82
n - C ₁₁	80.3623	2.8567	2.0186	9.0662	3.16	2.87
n - C ₁₂	81.8300	2.8726	2.0154	9.6555	3.22	2.82
i - C ₅	85.4721	2.9399	1.9438	4.5588	2.35	2.45
i - C ₈	82.0079	2.8945	1.9927	6.7031	2.92	2.79
c - C ₃	88.9329	2.8154	1.9281	3.1316	2.50	2.51
c - C ₆	97.3041	2.9248	1.9748	4.4789	2.16	2.63

References

- [1] CHAPMAN, W.G., JACKSON, G. and GUBBINS, K.E., *Molec. Phys.*, Vol. 65, **1988**, p.1057
- [2] HUANG, S.H. and RADOSZ, M., *Ind. Eng. Chem. Res.*, Vol. 29, **1990**, p.2284
- [3] TAVARES, F. W., CHANG, J. and SANDLER, S.I., *Molec. Phys.*, Vol. 86, **1995**, p.1451
- [4] PAREDES, M.L.L., NOBREGA, R. and TAVARES, F.W., *Ind. Eng. Chem. Res.*, Vol. 40, **2001**, p.1748
- [5] PAREDES, M.L.L., NOBREGA, R. and TAVARES, F.W., *Fluid Phase Equil.*, Vol. 179, **2001**, p.245
- [6] WERTHEIM, M.S., *J. Chem. Phys.*, Vol. 87, **1987**, p.7323
- [7] CHANG, J. and SANDLER, S., *Chem. Eng. Sci.*, Vol. 49, **1994**, p.2777
- [8] CARNAHAN, N.F. and STARLING, K.E., *J. Chem. Phys.*, Vol. 51, **1969**, p.635
- [9] CHIEW, Y.C., *J. Chem. Phys.*, Vol. 93, **1990**, p.5067
- [10] GHONASGI, D. and CHAPMAN, W.G., *J. Chem. Phys.*, Vol. 100, **1994**, p.6633
- [11] LIN, C.T., STELL, G. and KALYUZHNYI, Y.V., *J. Chem. Phys.*, Vol. 142, **2000**, p.3071
- [12] REID, R.C., PRAUSNITZ, J.M. and POLING, B.E., *The Properties of Gases and Liquids*, McGraw-Hill, 4th Ed., New York, **1987**.

Acknowledgements

M. L. L. Paredes wishes to thank FAPESP for the pos doc fellowship (00/07064-4). The authors thank FAPESP (1999/01962-1) for the financial support.